

ESTIMATING THE KIRBY-THOMPSON INVARIANTS OF SURFACE-LINKS IN THE YOSHIKAWA TABLE

MINAMI TANIGUCHI

ABSTRACT. In [Z23], minimal tri-plane diagrams of surface-links listed in the Yoshikawa table are computed using ch-diagrams. In this paper, we obtain upper bounds for the \mathcal{L} - and \mathcal{L}^* -invariants of several surface-links in the Yoshikawa table by using their tri-plane diagrams.

1. INTRODUCTION

In [MZ17], Meier–Zupan introduced a *bridge trisection* of a surface-link F in S^4 , which is a decomposition of (S^4, F) into three trivial disk systems. In this way, we obtain a new diagram of F called a *tri-plane diagram*, which is a tuple of planar diagrams of three trivial tangles representing the boundaries of the trivial disk systems of the bridge trisection. In [Z23], minimal tri-plane diagrams of all surface-links listed in the Yoshikawa table are computed, and their bridge numbers are specified.

In [BCTT22], Blair–Campisi–Taylor–Tomova defined the \mathcal{L} -*invariant* $\mathcal{L}(F)$ of a surface-link $F \subset S^4$ using minimal bridge trisections of F and the pants complex of the bridge surface of the bridge trisections, and they showed that any bridge trisection of a surface-link F is standard if $\mathcal{L}(F) = 0$. Using the dual curve complex of the bridge surface instead of the pants complex, Aranda–Pongtanapaisan–Zhang introduced the \mathcal{L}^* -*invariant* $\mathcal{L}^*(F)$, and they showed that any bridge trisection of a surface-link F is standard if $\mathcal{L}^*(F) \leq 2$. In other words, if $\mathcal{L}(F) = 0$ or $\mathcal{L}^*(F) \leq 2$, a surface-link F is smoothly trivial. We refer to both the \mathcal{L} - and \mathcal{L}^* -invariants as the *Kirby-Thompson invariants*, and these invariants measure the complexity of surface-links. On the other hand, there are a few examples of surface-links determined their values of the Kirby-Thompson invariants since it is not even straightforward to calculate upper bounds of these invariants because their definitions are so complicated.

In this article, we compute upper bounds for the Kirby-Thompson invariants of several surface-links listed in the Yoshikawa table.

Main Theorem (Theorem 3.1). The Kirby-Thompson invariants of several surface-links in the Yoshikawa table are determined or estimated as follows.

label	$6_1^{0,1}$	$7_1^{0,-2}$	$8_1^{-1,-1}$	9_1	$9_1^{1,-2}$	10_1^1	10_3	$10_1^{0,0,1}$	$10_1^{-2,-2}$
\mathcal{L}	15	$15 \sim 16$	$15 \sim 18$	$15 \sim 16$	~ 25	~ 24	$15 \sim 34$	~ 27	~ 26
\mathcal{L}^*	12	$12 \sim 13$	12	$12 \sim 13$	~ 19	~ 18	$12 \sim 34$	~ 21	~ 20

In [APTZ21] and [APZ23], the values of the invariants of surface-links 8_1 , $8_1^{1,1}$, 10_1 , and 10_2 are determined.

Question 1. Compute upper bounds for the Kirby-Thompson invariants of the other surface-links $9_1^{0,1}$, $10_1^{0,1}$, $10_2^{0,1}$, $10_1^{1,1}$, $10_1^{0,-2}$, $10_2^{0,-2}$, and $10_1^{-1,-1}$.

Acknowledgement. The author would like to express sincere gratitude to his supervisor, Hisaaki Endo, for his support and encouragement throughout this work.

2. PRELIMINARIES

In this section, we recall some concepts to define and calculate the Kirby-Thompson invariants of surface-links. First of all, we recall bridge trisections of surface-links in S^4 . Let F be a surface-link in S^4 , and

2020 *Mathematics Subject Classification.* Primary 57K10; Secondary 57K20.

Key words and phrases. Knotted surface, Bridge trisection, Kirby-Thompson invariant.

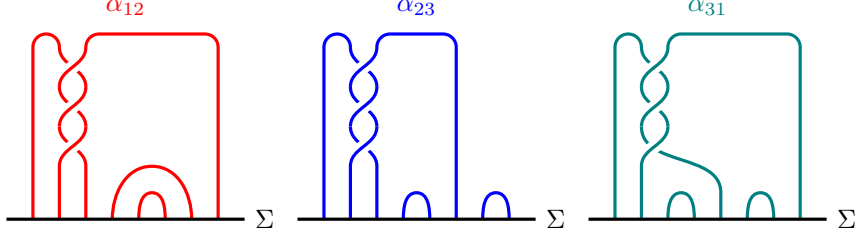


FIGURE 1. A tri-plane diagram of spun trefoil.

$X_1 \cup X_2 \cup X_3$ be a genus zero trisection of S^4 . For each $i, j \in \{1, 2, 3\}$, let $(X_i, \mathcal{D}_i) := (X_i, X_i \cap F)$, $(B_{ij}, \alpha_{ij}) := (X_i, \mathcal{D}_i) \cap (X_j, \mathcal{D}_j) = (\partial X_i, \partial \mathcal{D}_i) \cap (\partial X_j, \partial \mathcal{D}_j)$, and $(\Sigma, p) := (X_1, \mathcal{D}_1) \cap (X_2, \mathcal{D}_2) \cap (X_3, \mathcal{D}_3)$.

Definition 2.1. The decomposition $(S^4, F) = (X_1, \mathcal{D}_1) \cup (X_2, \mathcal{D}_2) \cup (X_3, \mathcal{D}_3)$ is said to be a $(b; c_1, c_2, c_3)$ -bridge trisection if it satisfies the following properties.

- (i) (X_i, \mathcal{D}_i) is a trivial c_i -disk system for each $i \in \{1, 2, 3\}$.
- (ii) (B_{ij}, α_{ij}) is a trivial b -tangle for each $i \neq j \in \{1, 2, 3\}$.
- (iii) (Σ, p) is a $2b$ -punctured 2-sphere, where $p = \alpha_{ij} \cap \Sigma = \alpha_{ij} \cap \alpha_{ki}$.

Let $(S^4, F) = (X_1, \mathcal{D}_1) \cup (X_2, \mathcal{D}_2) \cup (X_3, \mathcal{D}_3)$ be a $(b; c_1, c_2, c_3)$ -bridge trisection. From the above definition, each (B_{ij}, α_{ij}) is a trivial b -tangle, and the boundary sum $(B_{ij}, \alpha_{ij}) \cup_{\partial} \overline{(B_{ki}, \alpha_{ki})}$ is the unlink $(\partial X_i, \partial \mathcal{D}_i)$. We call the tuple of trivial b -tangles as a *tri-plane diagram* of the bridge trisection. For instance, a tri-plane diagram of the spun trefoil is shown in Figure 1. Refer to [APTZ21] for more detailed information on how to depict the diagram, and to [HKM20] for more detailed information on banded unlink diagrams.

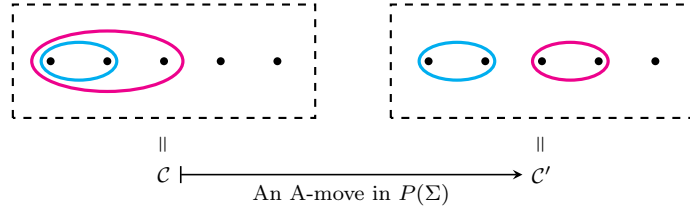
Secondly, we recall the definitions of the pants complex and the dual curve complex of a punctured 2-sphere. Let b be an integer with $b \geq 2$. Let $\Sigma = \Sigma_{2b,0}$ be a $2b$ -punctured 2-sphere, and $\mathcal{C} = \{c_1, \dots, c_{2b-3}\}$ be a collection of disjoint essential simple closed curves on Σ .

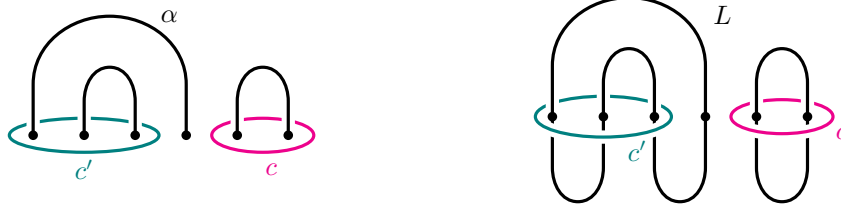
Definition 2.2.

- (i) \mathcal{C} is said to be a *pants decomposition* of Σ if we obtain $2b-2$ pairs of pants by cutting Σ along every essential curve $c \in \mathcal{C}$.
- (ii) Let $\mathcal{C} = \{c_1, \dots, c_{2b-3}\}$ and $\mathcal{C}' = \{c'_1, \dots, c'_{2b-3}\}$ be pants decompositions of Σ . \mathcal{C}' is obtained from \mathcal{C} by an *A-move* if they satisfy the following properties.
 - (I) For each $i \in \{1, \dots, 2b-2\}$, $c_i = c'_i$.
 - (II) $|c_{2b-3} \cap c'_{2b-3}| = 2$.
- Similarly, \mathcal{C}' is obtained from \mathcal{C} by an *A^* -move* if they satisfy the following properties.
 - (I) For each $i \in \{1, \dots, 2b-2\}$, $c_i = c'_i$.
 - (II) $|c_{2b-3} \cap c'_{2b-3}| \geq 2$.
- (iii) A 1-complex $P(\Sigma)$ is said to be the *pants complex* of Σ if it satisfies the following properties.
 - (I) A vertex of $P(\Sigma)$ is a pants decomposition \mathcal{C} of Σ .
 - (II) Two vertex $\mathcal{C}, \mathcal{C}' \in P(\Sigma)$ is connected by an *edge* in $P(\Sigma)$ if \mathcal{C}' is obtained from \mathcal{C} by an A-move.

Similarly, a 1-complex $C^*(\Sigma)$ is said to be the *dual curve complex* if it satisfies the following properties.

- (I) A vertex of $C^*(\Sigma)$ is a pants decomposition \mathcal{C} of Σ .

FIGURE 2. An example of pants decompositions \mathcal{C} and \mathcal{C}' of five punctured 2-sphere $\Sigma_{5,0}$ whose distance in $P(\Sigma)$ is equal to one.



(A) An example of a compressing curve c and a cut curve c' for a trivial 3-tangle α . (B) An example of a reducing curve c and a c -reducing curve c' for a 3-bridge split unlink L .

(II) Two vertices $\mathcal{C}, \mathcal{C}' \in C^*(\Sigma)$ is connected by an *edge* in $C^*(\Sigma)$ if \mathcal{C}' is obtained from \mathcal{C} by an A^* -move.

Let (B, α) be a trivial b -tangle and $(\Sigma, p) = (\partial B, \partial \alpha)$ the $2b$ -punctured 2-sphere. Let c be an essential simple closed curve on Σ .

Definition 2.3.

- (i) The curve c is said to be *compressing* if there exists a 2-disk $D \subset B$ such that $\partial D = c$ and $|D \cap \alpha| = 0$. We refer to such a 2-disk D as a *compressing disk* for the tangle (B, α) .
- (ii) The curve c is said to be *cut* if there exists a 2-disk $D \subset B$ such that $\partial D = c$ and $|D \cap \alpha| = 1$. We refer to such a 2-disk D as a *cut disk* for the tangle (B, α) .

Let (S^3, L) be a b -bridge split unlink $(B_+, \alpha_+) \cup_{\partial} (\overline{B_-, \alpha_-})$, where each (B_{\pm}, α_{\pm}) is a trivial b -tangle, and $(\Sigma, p) = (\partial B_{\pm}, \partial \alpha_{\pm})$ the $2b$ -punctured 2-sphere. Let c be an essential simple closed curve on Σ .

Definition 2.4.

- (i) The curve c is said to be *reducing* if there exists a 2-sphere $Q \subset S^3$ such that $Q \cap \Sigma = c$ and $|Q \cap L| = 0$. We refer to such a 2-sphere Q as a *reducing sphere* for the unlink (S^3, L) . We note that each 2-disk $Q \cap B_{\pm} \subset B_{\pm}$ is also compressing for the tangle (B_{\pm}, α_{\pm}) , respectively.
- (ii) The curve c is said to be *c-reducing* if there exists a 2-sphere $Q \subset S^3$ such that $Q \cap \Sigma = c$ and $|Q \cap \alpha_+| = |Q \cap \alpha_-| = 1$. We refer to such a 2-sphere Q as a *c-reducing sphere* for the unlink (S^3, L) . We note that each 2-disk $Q \cap B_{\pm} \subset B_{\pm}$ is also cut for the tangle (B_{\pm}, α_{\pm}) , respectively.

With these preliminaries, we define the Kirby-Thompson invariants of a surface-link. Let $F \subset S^4$ be a surface-link and $(S^4, F) = (X_1, \mathcal{D}_1) \cup (X_2, \mathcal{D}_2) \cup (X_3, \mathcal{D}_3)$ a minimal $(b; c_1, c_2, c_3)$ -bridge trisection of F . Let \mathcal{T} denote the bridge trisection. Let $(\Sigma, p) = (X_1, \mathcal{D}_1) \cap (X_2, \mathcal{D}_2) \cap (X_3, \mathcal{D}_3)$ be the bridge surface of the bridge trisection, and we regard the bridge surface as a $2b$ -punctured 2-sphere. Let $D_c(\alpha_{ij})$ denote the set of vertices of $P(\Sigma)$ whose curves are either compressing or cut curves for the trivial b -tangle (B_{ij}, α_{ij}) .

Definition 2.5.

- (i) A pair of efficient pants decompositions $(p_{ij}^i, p_{ki}^i) \in D_c(\alpha_{ij}) \times D_c(\alpha_{ki})$ is said to be an *efficient defining pair* for the unlink $\partial \mathcal{D}_i$ if the distance between p_{ij}^i and p_{ki}^i in $P(\Sigma)$ (or in $C^*(\Sigma)$) is equal to $b - c_i$.
- (ii) We define the \mathcal{L} -*invariant* $\mathcal{L}(\mathcal{T})$ of the bridge trisection \mathcal{T} as

$$\mathcal{L}(\mathcal{T}) := \min \left\{ \sum_{i,j} d^P(p_{ij}^i, p_{ij}^j) \mid \begin{array}{l} (p_{ij}^i, p_{ij}^j) \in D_c(\alpha_{ij}) \times D_c(\alpha_{ki}) \text{ is} \\ \text{an efficient defining pair for } \partial \mathcal{D}_i. \end{array} \right\},$$

where $d^P: P(\Sigma) \times P(\Sigma) \rightarrow \mathbb{Z}_{\geq 0}$ is the metric function of $P(\Sigma)$.

- (iii) We define the \mathcal{L} -*invariant* $\mathcal{L}(F)$ of the surface-link F as follows.

$$\mathcal{L}(F) := \min \{ \mathcal{L}(\mathcal{T}) \mid \mathcal{T} \text{ is a } b\text{-bridge trisection of } F. \}.$$

Using the dual curve complex $C^*(\Sigma)$ instead of the pants complex $P(\Sigma)$, we can define another invariant \mathcal{L}^* as follows.

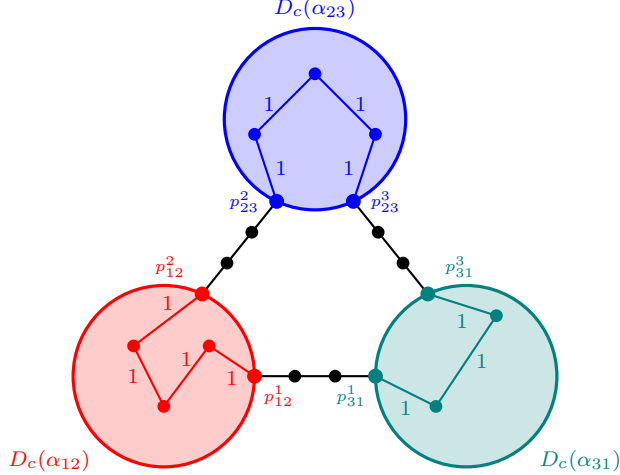


FIGURE 4. An image of the Kirby-Thompson invariants, where each (p_{ij}^i, p_{ki}^i) is an efficient defining pair for the unlink $\partial\mathcal{D}_i$.

(iv) We define the \mathcal{L}^* -invariant $\mathcal{L}^*(\mathcal{T})$ of the bridge trisection \mathcal{T} as

$$\mathcal{L}^*(\mathcal{T}) := \min \left\{ \sum_{i,j} d^*(p_{ij}^i, p_{ij}^j) \mid \begin{array}{l} (p_{ij}^i, p_{ki}^i) \in D_c(\alpha_{ij}) \times D_c(\alpha_{ki}) \text{ is} \\ \text{an efficient defining pair for } \partial\mathcal{D}_i. \end{array} \right\},$$

where $d^*: C^*(\Sigma) \times C^*(\Sigma) \rightarrow \mathbb{Z}_{\geq 0}$ is the metric function of $C^*(\Sigma)$.

(v) We define the \mathcal{L}^* -invariant $\mathcal{L}^*(F)$ of the surface-link F as follows.

$$\mathcal{L}^*(F) := \min \{ \mathcal{L}^*(\mathcal{T}) \mid \mathcal{T} \text{ is a } b\text{-bridge trisection of } F. \}.$$

We refer to both the \mathcal{L} -invariant and the \mathcal{L}^* -invariant as the *Kirby-Thompson invariants*.

The following properties of the Kirby-Thompson invariants are fundamental.

Theorem 2.1 ([BCTT22], [APZ23]). *Let F be a surface-link in S^4 , then the following properties hold.*

- (i) $\mathcal{L}^*(F), \mathcal{L}(F) \in \mathbb{Z}_{\geq 0}$, $\mathcal{L}^*(F) \leq \mathcal{L}(F)$.
- (ii) *If $\mathcal{L}(F) = 0$ holds, the surface-link F is smoothly isotopic to the distant sum of the connected sum of finitely many standard surfaces.*
- (iii) *If $\mathcal{L}^*(F) \leq 2$ holds, the surface-link F is smoothly isotopic to the distant sum of the connected sum of finitely many standard surfaces.*

In other words, the Kirby-Thompson invariants can specify whether a surface-link is smoothly unlinked or not. Furthermore, in [APZ23], some lower bounds for these invariants are provided for irreducible and unstabilized bridge trisections.

Lemma 2.1 ([APZ23]). *Let \mathcal{T} be an irreducible and unstabilized $(b; c)$ -bridge trisection for a surface-link F . Then,*

- (i) $\mathcal{L}(\mathcal{T}) \geq \mathcal{L}^*(\mathcal{T}) \geq 3(b + c - 3)$.
- (ii) $(b, c) = (4, 2) \implies \mathcal{L}^*(\mathcal{T}) \geq 12$.
- (iii) $c \geq 2 \implies \mathcal{L}(\mathcal{T}) \geq 3(b + c - 2)$.
- (iv) $c = 2 \implies \mathcal{L}(\mathcal{T}) \geq 3(b + 1)$.

3. MAIN RESULT

In this section, we prove the following main theorem. We note that, in all of the following figures, all compressing or cut curves for tangles α_{12} , α_{23} , and α_{31} are depicted in red, blue, and green, respectively, and all common curves in $p_{ij}^i \cap p_{ki}^k$ are depicted in orange for each $\{i, j, k\} = \{1, 2, 3\}$.

Theorem 3.1. *The Kirby-Thompson invariants of several surface-links in the Yoshikawa table are determined or estimated as follows.*

label	$6_1^{0,1}$	$7_1^{0,-2}$	$8_1^{-1,-1}$	9_1	$9_1^{1,-2}$	10_1^1	10_3	$10_1^{0,0,1}$	$10_1^{-2,-2}$
\mathcal{L}	15	$15 \sim 16$	$15 \sim 18$	$15 \sim 16$	~ 25	~ 24	$15 \sim 34$	~ 27	~ 26
\mathcal{L}^*	12	$12 \sim 13$	12	$12 \sim 13$	~ 19	~ 18	$12 \sim 34$	~ 21	~ 20

Proof. From lemma 3.1, lemma 3.2, lemma 3.3, lemma 3.4, lemma 3.5, lemma 3.6, lemma 3.7, lemma 3.8, and lemma 3.9, we obtain upper bounds for the Kirby-Thompson invariants of the surface-links listed in the above table. On the other hand, since any minimal $(4; 2)$ -bridge trisection is irreducible, from lemma 2.1, we obtain lower bounds for the Kirby-Thompson invariants of surface-links whose bridge number are four. \square

In [APZ23], any $(6; 2)$ -minimal bridge trisection of T^2 -spin of nontrivial 2-bridge link is irreducible. If any minimal bridge trisection with bridge number less than or equal to six is irreducible, we obtain stricter evaluations for the invariants of the surface-links in theorem 3.1.

Question 2. *Is any minimal bridge trisection with bridge number less than or equal to six irreducible?*

Lemma 3.1. *The following inequalities hold.*

$$\mathcal{L}(6_1^{0,1}) \leq 15, \mathcal{L}^*(6_1^{0,1}) \leq 12$$

Proof. From [Z23], a tri-plane diagram of $6_1^{0,1}$ is as in Figure 5. From the tri-plane diagram in Figure 5, we can find efficient defining pairs for the bridge trisection of $6_1^{0,1}$ shown in Figure 6. We can see that

$$d^P(p_{ij}^i, p_{ij}^j) \leq 5$$

for each $i, j \in \{1, 2, 3\}$, hence $\mathcal{L}(6_1^{0,1}) \leq 5 + 5 + 5 = 15$ holds. In the same way, from Figure 7, we see that

$$d^*(p_{ij}^i, p_{ij}^j) \leq 4$$

for each $i, j \in \{1, 2, 3\}$, hence $\mathcal{L}^*(6_1^{0,1}) \leq 4 + 4 + 4 = 12$ holds. \square

Lemma 3.2. *The following inequalities hold.*

$$\mathcal{L}(7_1^{0,-2}) \leq 16, \mathcal{L}^*(7_1^{0,-2}) \leq 13$$

Proof. From [Z23], a tri-plane diagram of $7_1^{0,-2}$ is as in Figure 8. From the tri-plane diagram in Figure 8, we can find efficient defining pairs for the bridge trisection of $7_1^{0,-2}$ shown in Figure 9. We can see that

$$d^P(p_{12}^1, p_{12}^2) \leq 4, d^P(p_{23}^2, p_{23}^3) \leq 4, d^P(p_{31}^3, p_{31}^1) \leq 5$$

for each $i, j \in \{1, 2, 3\}$, hence $\mathcal{L}(7_1^{0,-2}) \leq 4 + 4 + 5 = 13$ holds. In the same way, from Figure 10, we see that

$$d^*(p_{12}^1, p_{12}^2) \leq 4, d^*(p_{23}^2, p_{23}^3) \leq 4, d^*(p_{31}^3, p_{31}^1) \leq 5,$$

hence $\mathcal{L}^*(7_1^{0,-2}) \leq 4 + 4 + 5 = 13$ holds. \square

Question 3. *Does there exist some bridge trisection of $7_1^{0,-2}$ together with efficient defining pairs such that $\mathcal{L}(7_1^{0,-2}) \leq 15, \mathcal{L}^*(7_1^{0,-2}) \leq 12$?*

Lemma 3.3. *The following inequalities hold.*

$$\mathcal{L}(8_1^{-1,-1}) \leq 18, \mathcal{L}^*(8_1^{-1,-1}) \leq 12$$

Proof. From [Z23], a tri-plane diagram of $8_1^{-1,-1}$ is as in Figure 11. From the tri-plane diagram in Figure 11, we can find efficient defining pairs for the bridge trisection of $8_1^{-1,-1}$ shown in Figure 12. We see that

$$d^P(p_{ij}^i, p_{ij}^j) \leq 6$$

for each $i, j \in \{1, 2, 3\}$, hence $\mathcal{L}(8_1^{-1,-1}) \leq 6 + 6 + 6 = 18$ holds. In the same way, from Figure 13, we see that

$$d^*(p_{ij}^i, p_{ij}^j) \leq 4$$

for each $i, j \in \{1, 2, 3\}$, hence $\mathcal{L}^*(8_1^{-1,-1}) \leq 4 + 4 + 4 = 12$ holds. \square

Lemma 3.4. *The following inequalities hold.*

$$\mathcal{L}(9_1) \leq 16, \mathcal{L}^*(9_1) \leq 13$$

Proof. From [Z23], a tri-plane diagram of 9_1 is as in Figure 14. From the tri-plane diagram in Figure 14, we can find efficient defining pairs for the bridge trisection of 9_1 shown in Figure 15. We see that

$$d^P(p_{12}^1, p_{12}^2) \leq 5, d^P(p_{23}^2, p_{23}^3) \leq 5, d^P(p_{31}^3, p_{31}^1) \leq 6,$$

hence $\mathcal{L}(9_1) \leq 5 + 5 + 6 = 16$ holds. In the same way, from Figure 16, we see that

$$d^*(p_{12}^1, p_{12}^2) \leq 4, d^*(p_{23}^2, p_{23}^3) \leq 4, d^*(p_{31}^3, p_{31}^1) \leq 5,$$

hence $\mathcal{L}^*(9_1) \leq 4 + 4 + 5 = 13$ holds. \square

Question 4. *Does there exist some bridge trisection of 9_1 together with efficient defining pairs such that $\mathcal{L}(9_1) \leq 15$, $\mathcal{L}^*(9_1) \leq 12$?*

Lemma 3.5. *The following inequations hold.*

$$\mathcal{L}(9_1^{1,-2}) \leq 25, \mathcal{L}^*(9_1^{1,-2}) \leq 19$$

Proof. From [Z23], a tri-plane diagram of $9_1^{1,-2}$ is as in Figure 17. From the tri-plane diagram in Figure 17, we can find efficient defining pairs for the bridge trisection of $9_1^{1,-2}$ shown in Figure 18. We see that

$$d^P(p_{12}^1, p_{12}^2) \leq 9, d^P(p_{23}^2, p_{23}^3) \leq 8, d^P(p_{31}^3, p_{31}^1) \leq 8,$$

hence $\mathcal{L}(9_1^{1,-2}) \leq 9 + 8 + 8 = 25$ holds. In the same way, from Figure 19, we see that

$$d^*(p_{12}^1, p_{12}^2) \leq 7, d^*(p_{23}^2, p_{23}^3) \leq 6, d^*(p_{31}^3, p_{31}^1) \leq 6,$$

hence $\mathcal{L}^*(9_1^{1,-2}) \leq 7 + 6 + 6 = 19$ holds. \square

Question 5. *Does there exist some bridge trisection of $9_1^{1,-2}$ together with efficient defining pairs such that $\mathcal{L}(9_1^{1,-2}) \leq 24$, $\mathcal{L}^*(9_1^{1,-2}) \leq 18$?*

Lemma 3.6. *The following inequations hold.*

$$\mathcal{L}(10_1^1) \leq 24, \mathcal{L}^*(10_1^1) \leq 18$$

Proof. From [Z23], a tri-plane diagram of 10_1^1 is as in Figure 20. From the tri-plane diagram in Figure 20, we can find efficient defining pairs for the bridge trisection of 10_1^1 shown in Figure 21. We see that

$$d^P(p_{ij}^i, p_{ij}^j) \leq 8$$

for each $i, j \in \{1, 2, 3\}$, hence $\mathcal{L}(10_1^1) \leq 8 + 8 + 8 = 24$ holds. In the same way, from Figure 22, we see that

$$d^*(p_{ij}^i, p_{ij}^j) \leq 6$$

for each $i, j \in \{1, 2, 3\}$, hence $\mathcal{L}^*(10_1^1) \leq 6 + 6 + 6 = 18$ holds. \square

The efficient defining pairs for the minimal tri-plane diagram of 10_3 , constructed in Figure 24, are so complicated that we cannot find any shorter paths in $C^*(\Sigma)$.

Lemma 3.7. *The following inequations hold.*

$$\mathcal{L}^*(10_3) \leq \mathcal{L}(10_3) \leq 34$$

Proof. From [Z23], a tri-plane diagram of 10_3 is as in Figure 23. From the tri-plane diagram in Figure 23, we can find efficient defining pairs for the bridge trisection of 10_3 shown in Figure 24. We see that

$$d^P(p_{12}^1, p_{12}^2) \leq 13, d^P(p_{23}^2, p_{23}^3) \leq 8, d^P(p_{31}^3, p_{31}^1) \leq 13,$$

hence $\mathcal{L}(10_3) \leq 13 + 8 + 13 = 34$ holds. \square

Question 6. *Find a sequence of A-moves realizing minimal distance of $p_{ij}^i \rightarrow p_{ij}^j$ in $C^*(\Sigma)$ for each $i \neq j \in \{1, 2, 3\}$. Furthermore, find alternative efficient defining pairs for the bridge trisection of 10_3 that give stricter upper bounds of $\mathcal{L}(10_3)$ and $\mathcal{L}^*(10_3)$.*

Lemma 3.8. *The following inequations hold.*

$$\mathcal{L}(10_1^{0,0,1}) \leq 27, \mathcal{L}^*(10_1^{0,0,1}) \leq 21$$

Proof. From [Z23], a tri-plane diagram of $10_1^{0,0,1}$ is as in Figure 25. From the tri-plane diagram in Figure 25, we can find efficient defining pairs for the bridge trisection of $10_1^{0,0,1}$ shown in Figure 26. We see that

$$d^P(p_{ij}^i, p_{ij}^j) \leq 9$$

for each $i, j \in \{1, 2, 3\}$, hence $\mathcal{L}(10_1^{0,0,1}) \leq 9 + 9 + 9 = 27$ holds. In the same way, from Figure 27, we see that

$$d^*(p_{ij}^i, p_{ij}^j) \leq 7$$

for each $i, j \in \{1, 2, 3\}$, hence $\mathcal{L}^*(10_1^{0,0,1}) \leq 7 + 7 + 7 = 21$ holds. \square

Lemma 3.9. *The following inequalities hold.*

$$\mathcal{L}(10_1^{-2,-2}) \leq 26, \mathcal{L}^*(10_1^{-2,-2}) \leq 20$$

Proof. From [Z23], a tri-plane diagram of $10_1^{-2,-2}$ is as in Figure 28. From the tri-plane diagram in Figure 28, we can find efficient defining pairs for the bridge trisection of $10_1^{-2,-2}$ shown in Figure 29. We see that

$$d^P(p_{12}^1, p_{12}^2) \leq 10, d^P(p_{23}^2, p_{23}^3) \leq 8, d^P(p_{31}^3, p_{31}^1) \leq 8,$$

hence $\mathcal{L}(10_1^{-2,-2}) \leq 10 + 8 + 8 = 26$ holds. In the same way, from Figure 30, we see that

$$d^*(p_{12}^1, p_{12}^2) \leq 8, d^*(p_{23}^2, p_{23}^3) \leq 6, d^*(p_{31}^3, p_{31}^1) \leq 6,$$

hence $\mathcal{L}^*(10_1^{-2,-2}) \leq 8 + 6 + 6 = 20$ holds. \square

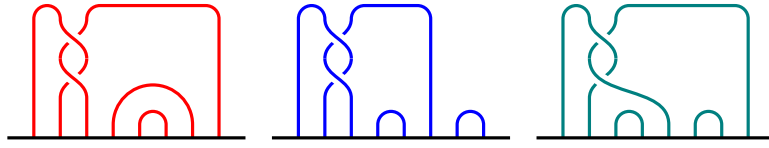
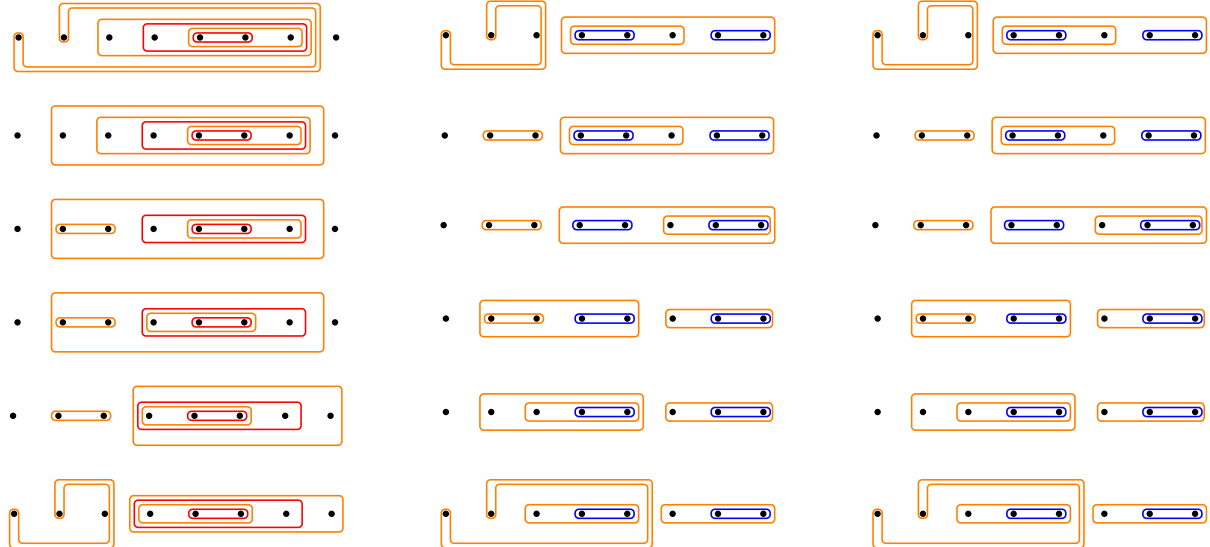
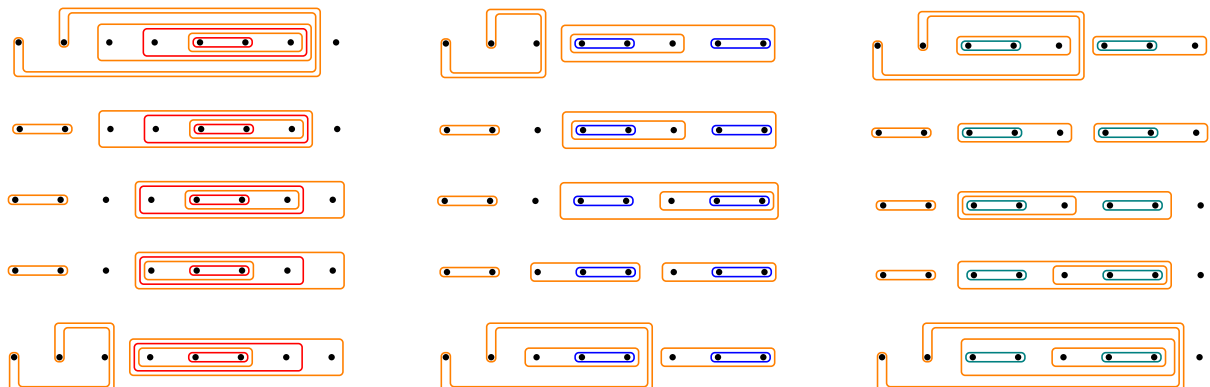
Question 7. *Does there exist some bridge trisection of $10_1^{-2,-2}$ together with efficient defining pairs such that $\mathcal{L}(10_1^{-2,-2}) \leq 24$, $\mathcal{L}^*(10_1^{-2,-2}) \leq 18$?*

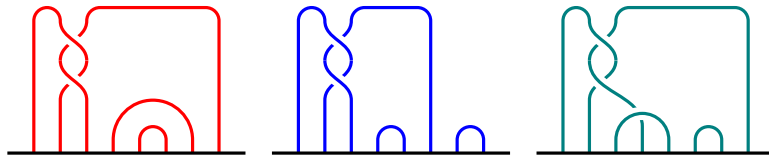
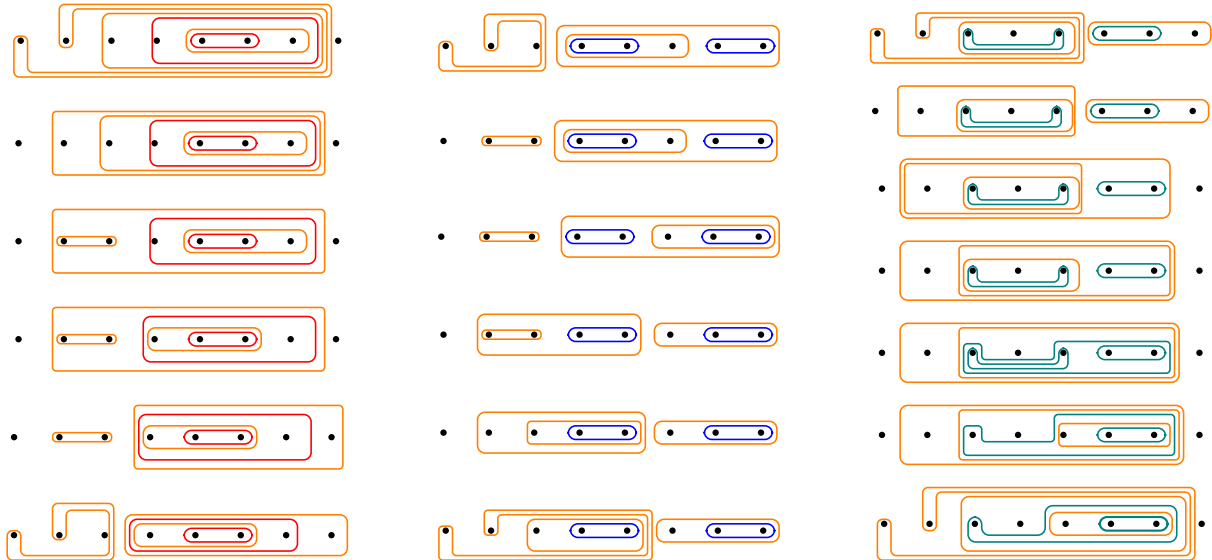
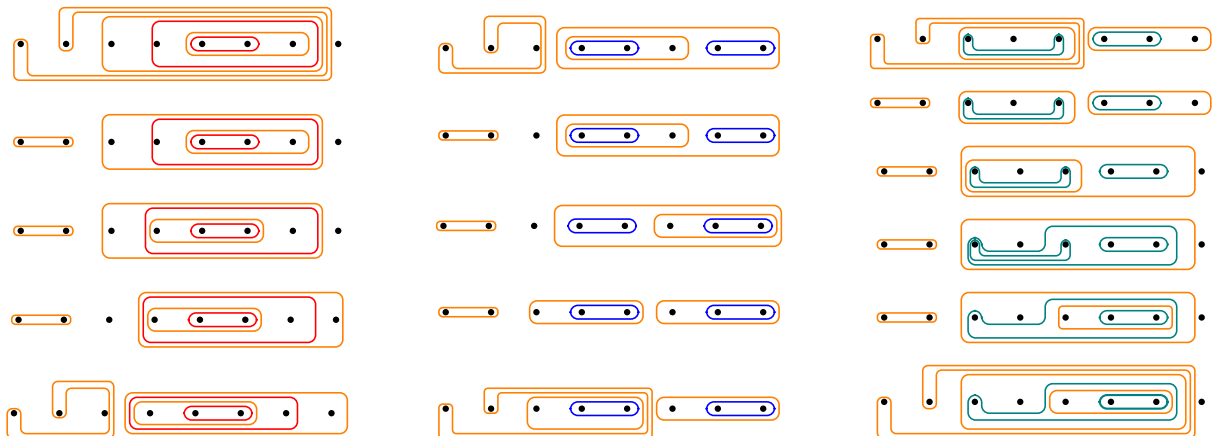
These lemmas suggest that the Kirby-Thompson invariants of surface-links may take values that are not multiples of three, although all the values of the invariants specified so far are divisible by three.

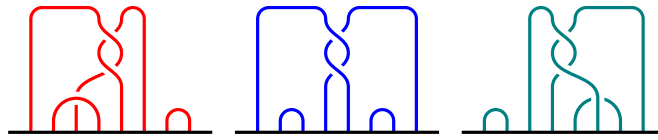
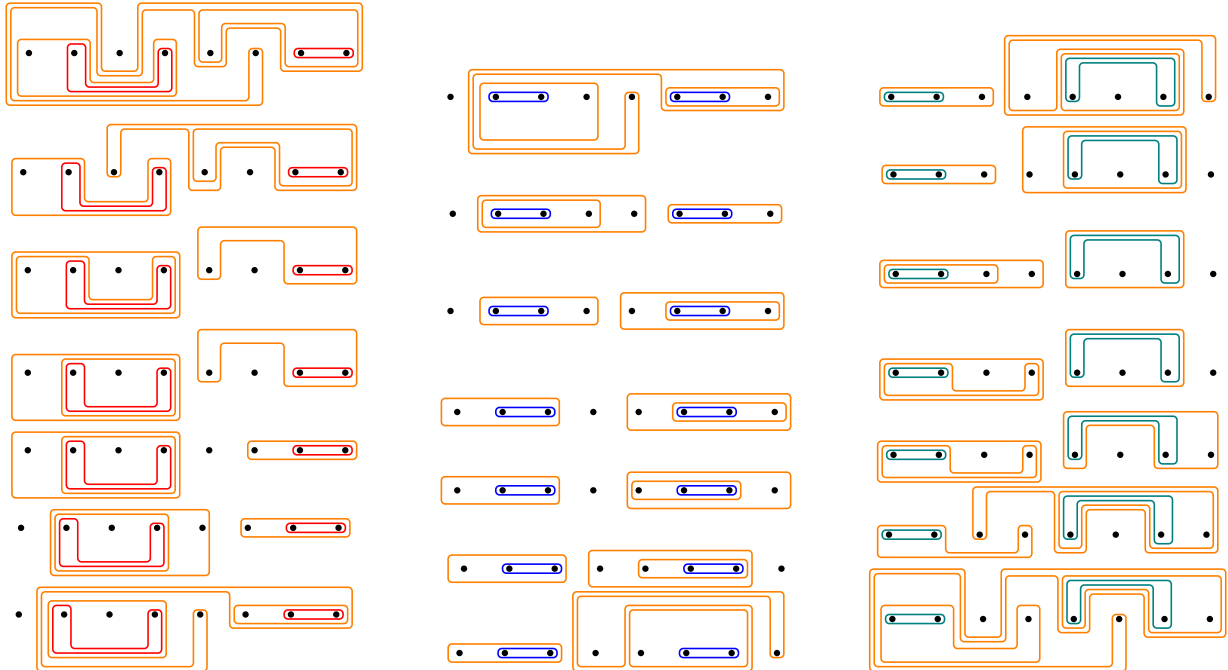
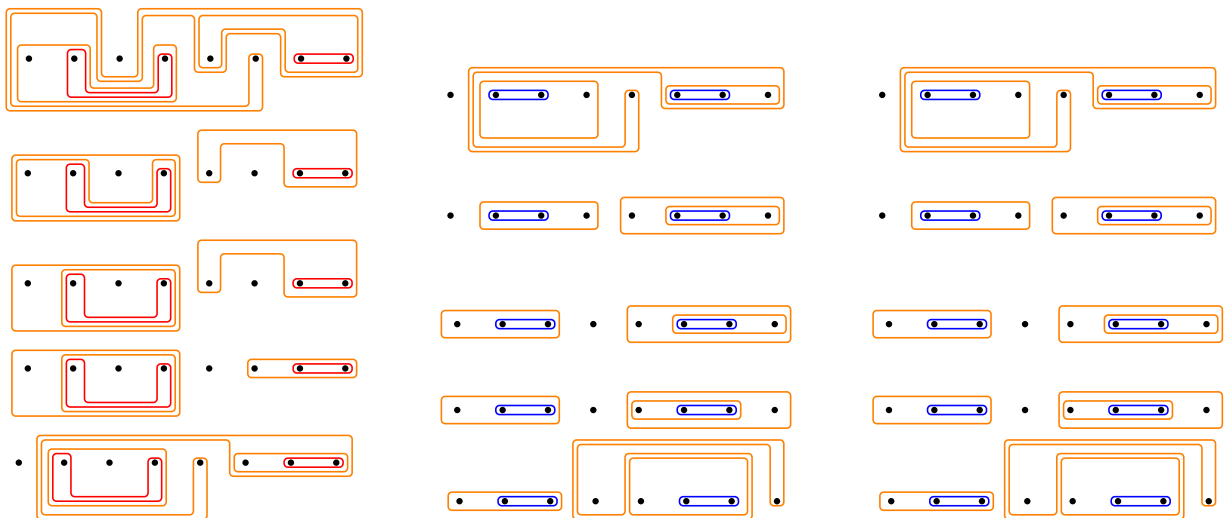
Question 8. *Do $\mathcal{L}(F) \equiv 0$, $\mathcal{L}^*(F) \equiv 0 \pmod{3}$ always hold for any surface-link F ?*

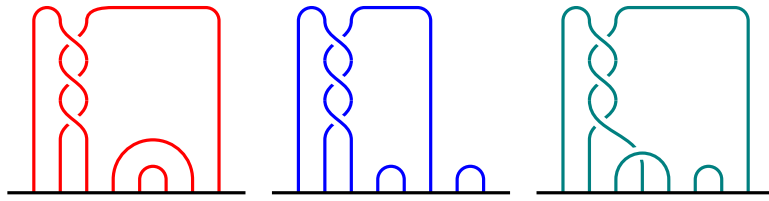
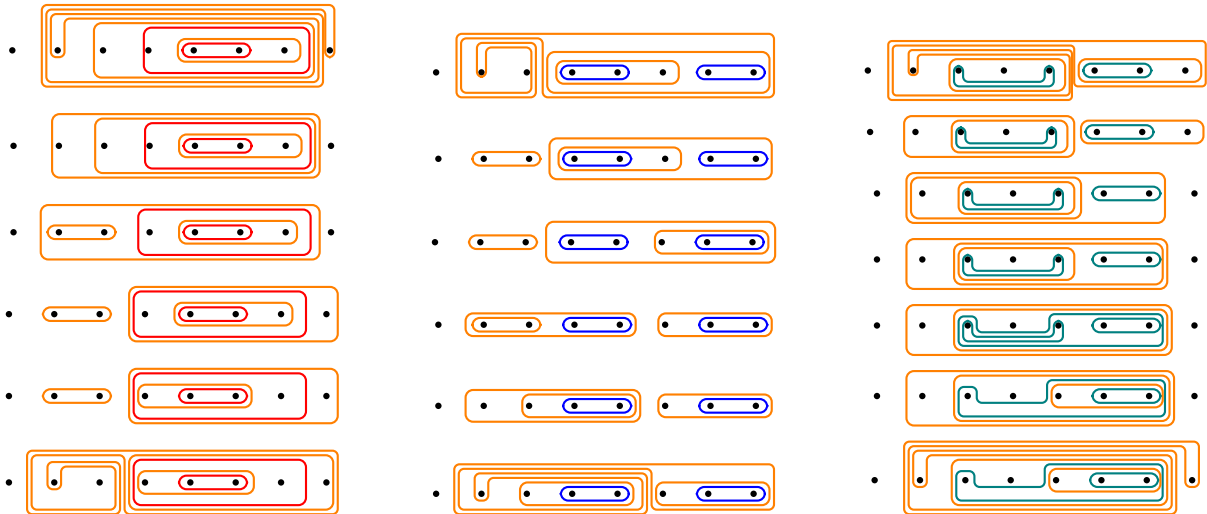
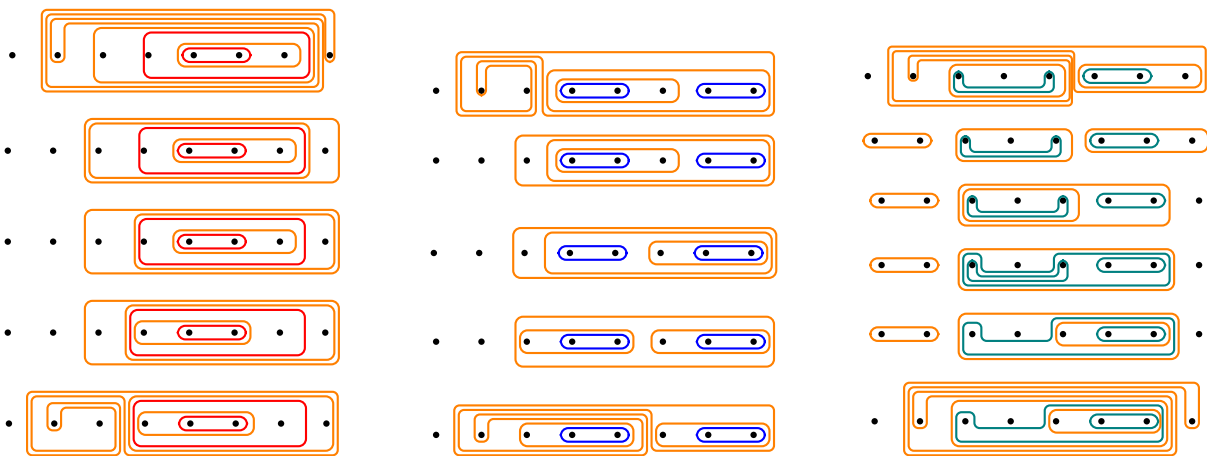
REFERENCES

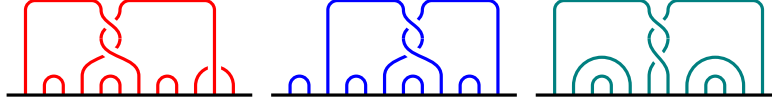
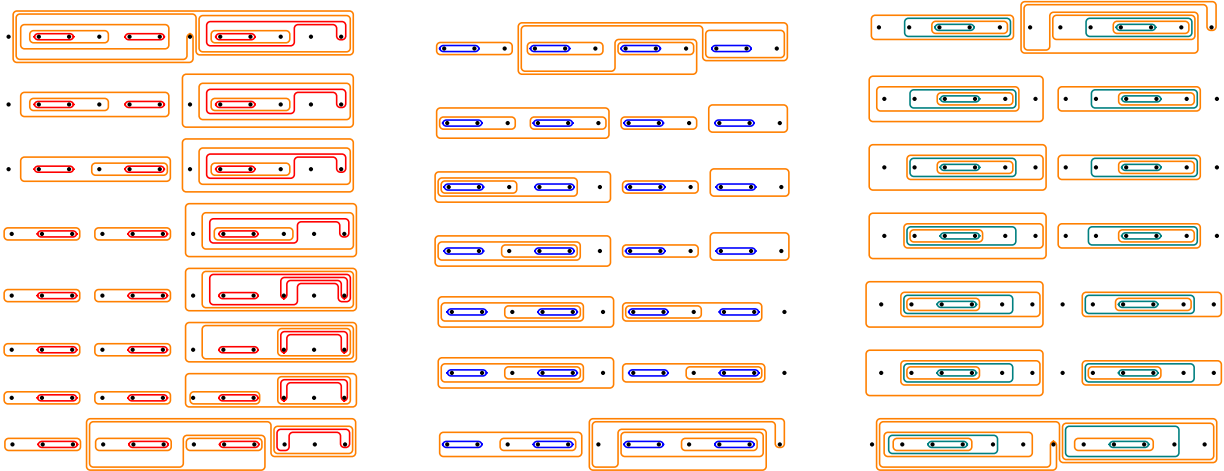
- [APTZ21] Román Aranda, Putting Pongtanapaisan, Scott A. Taylor, and Suixin Zhang. Bounding the kirby-thompson invariant of spun knots. *preprint, arXiv:2112.02420*, 2021.
- [APZ23] Román Aranda, Puttipong Pongtanapaisan, and Cindy Zhang. Bounds for Kirby-Thompson invariants of knotted surfaces. *Geom. Dedicata*, 217(6):Paper No. 99, 30, 2023.
- [BCTT22] Ryan Blair, Marion Campisi, Scott A. Taylor, and Maggy Tomova. Kirby-Thompson distance for trisections of knotted surfaces. *J. Lond. Math. Soc. (2)*, 105(2):765–793, 2022.
- [GK16] David Gay and Robion Kirby. Trisectioning 4-manifolds. *Geom. Topol.*, 20(6):3097–3132, 2016.
- [HKM20] Mark C. Hughes, Seungwon Kim, and Maggie Miller. Isotopies of surfaces in 4-manifolds via banded unlink diagrams. *Geom. Topol.*, 24(3):1519–1569, 2020.
- [MZ17] Jeffrey Meier and Alexander Zupan. Bridge trisections of knotted surfaces in S^4 . *Trans. Amer. Math. Soc.*, 369(10):7343–7386, 2017.
- [Z23] Allred, Wolfgang and Aragón, Manuel and Dooley, Zack and Goldman, Alexander and Lei, Yucong and Martinez, Isaiah and Meyer, Nicholas and Peters, Devon and Warrander, Scott and Wright, Ana and Zupan, Alexander. Tri-plane diagrams for simple surfaces in S^4 . *J. Knot Theory Ramif.*, 32(14):2350041, 28 pp., 2023.

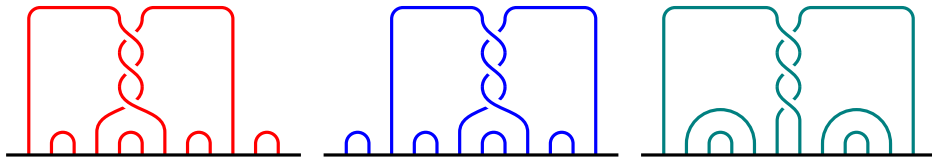
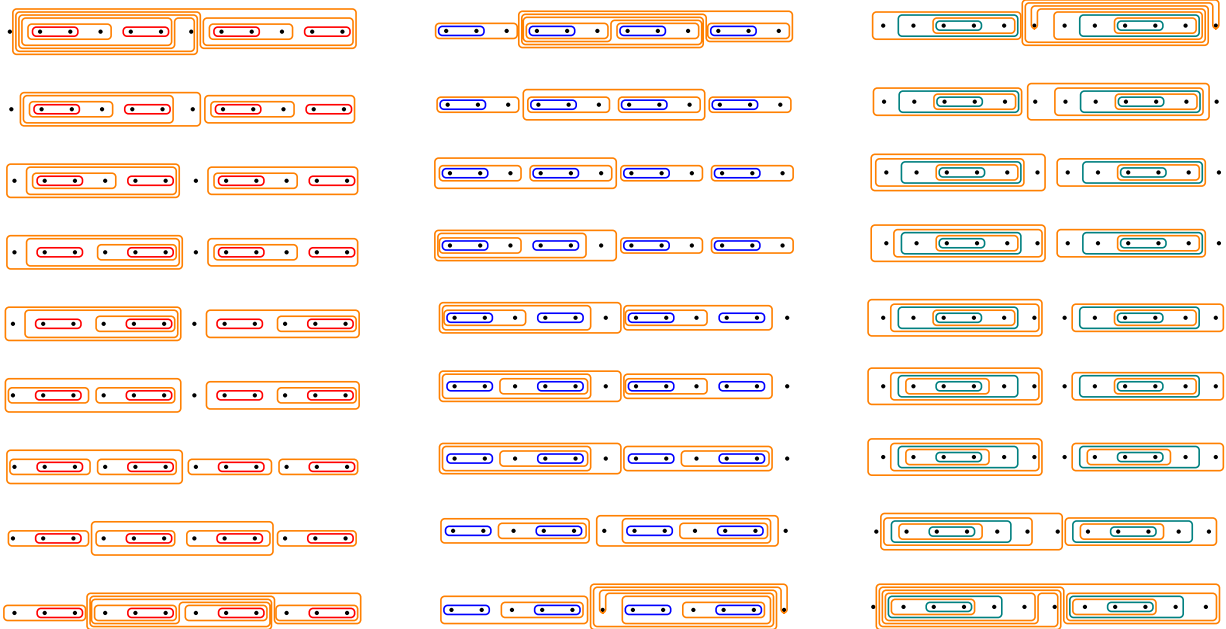
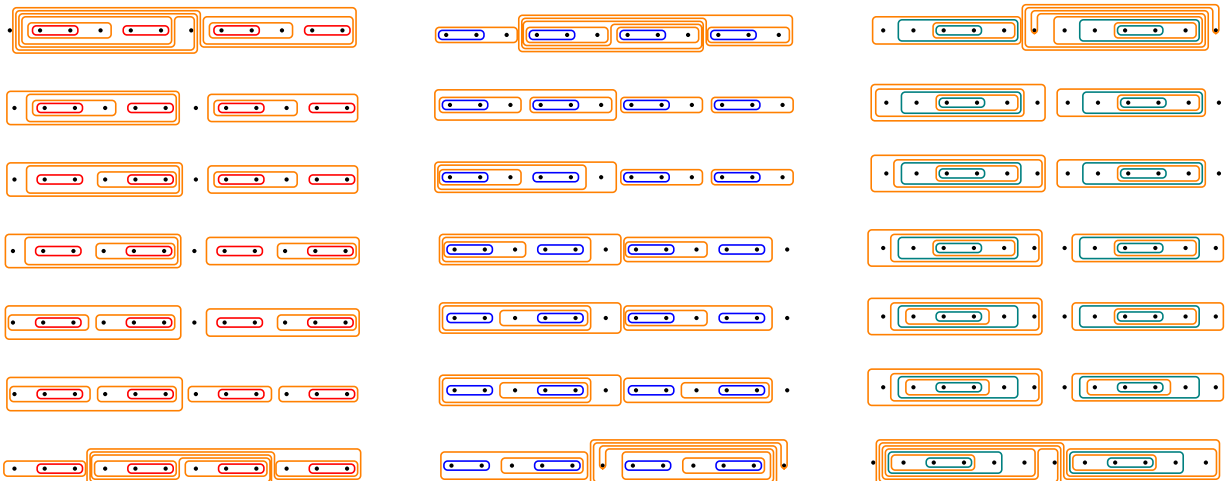
FIGURE 5. A tri-plane diagram of $6_1^{0,1}$.FIGURE 6. An upper bound for the \mathcal{L} -invariant of $6_1^{0,1}$.FIGURE 7. An upper bound for the \mathcal{L}^* -invariant of $6_1^{0,1}$.

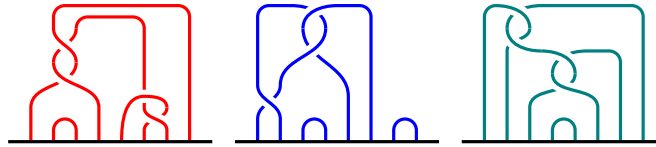
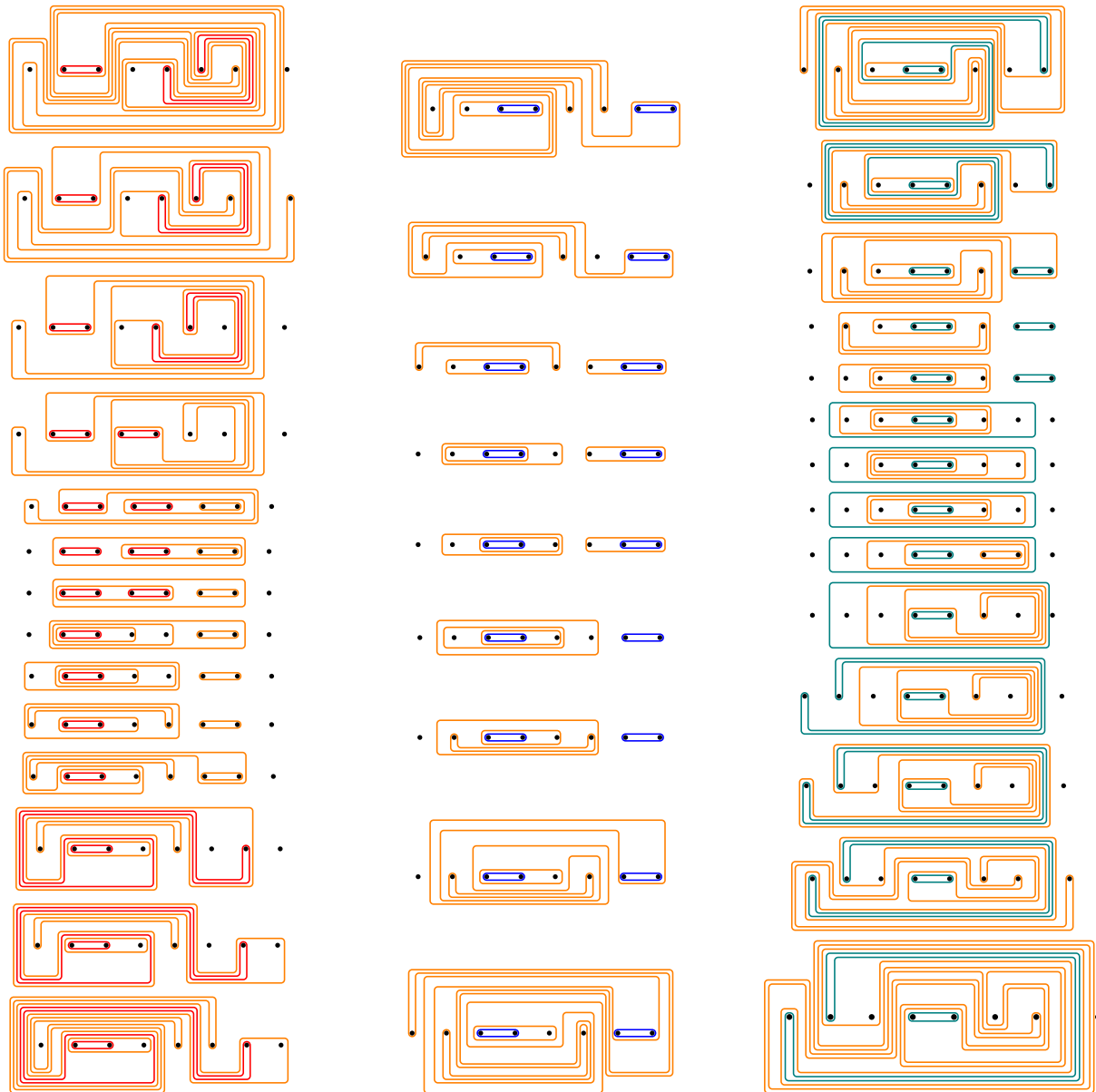
FIGURE 8. A tri-plane diagram of $7_1^{0,-2}$.FIGURE 9. An upper bound for the \mathcal{L} -invariant of $7_1^{0,-2}$.FIGURE 10. An upper bound for the \mathcal{L}^* -invariant of $7_1^{0,-2}$.

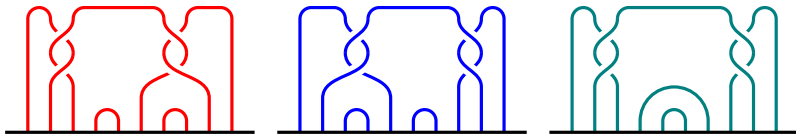
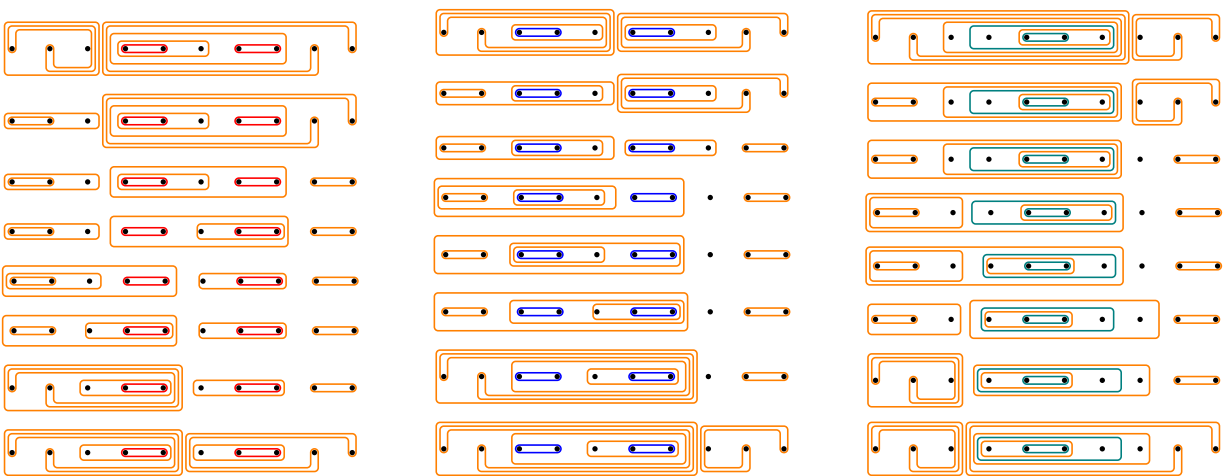
FIGURE 11. A tri-plane diagram of $8_1^{-1,-1}$.FIGURE 12. An upper bound for the \mathcal{L} -invariant of $8_1^{-1,-1}$.FIGURE 13. An upper bound for the \mathcal{L}^* -invariant of $8_1^{-1,-1}$.

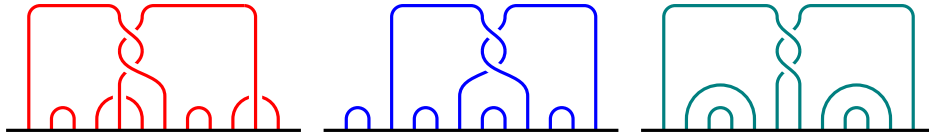
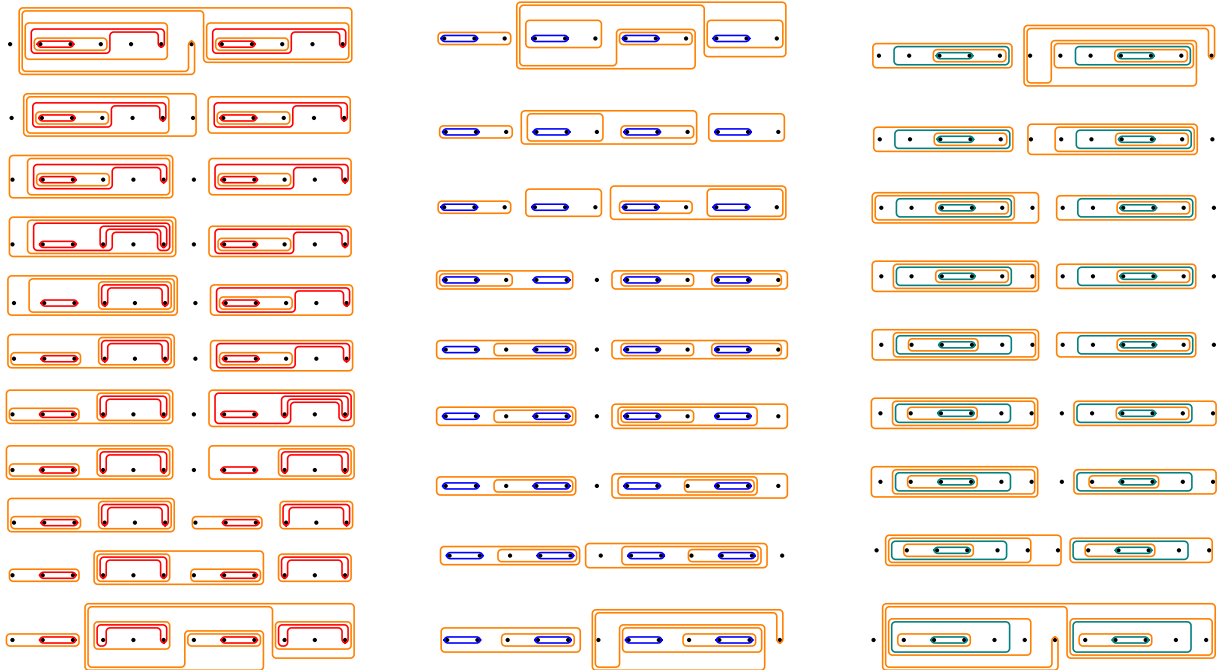
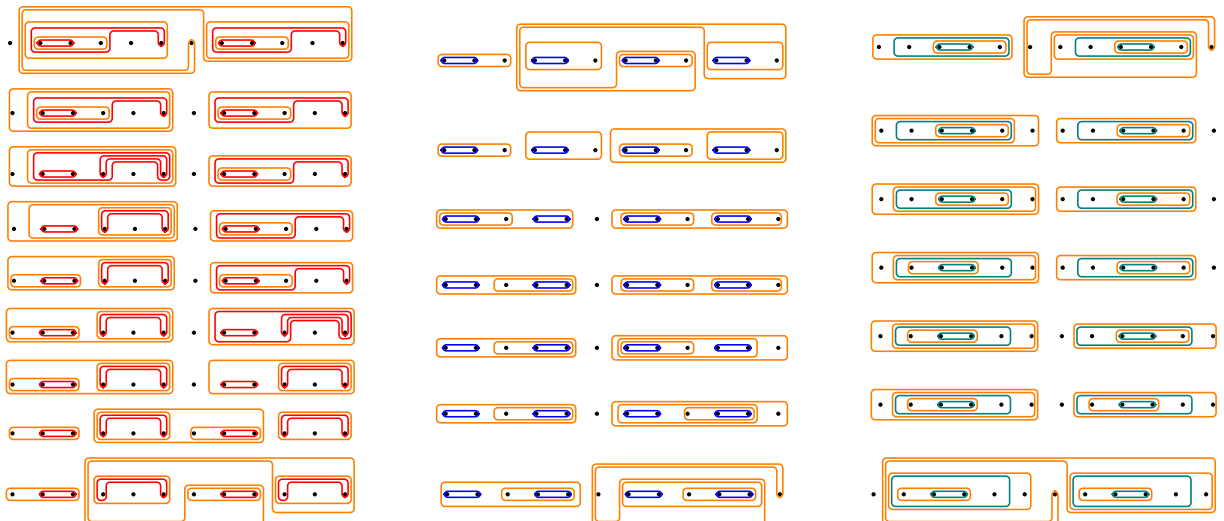
FIGURE 14. A tri-plane diagram of 9_1 .FIGURE 15. An upper bound for the \mathcal{L} -invariant of 9_1 .FIGURE 16. An upper bound for the \mathcal{L}^* -invariant of 9_1 .

FIGURE 17. A tri-plane diagram of $9_1^{1,-2}$.FIGURE 18. An upper bound for the \mathcal{L} -invariant of $9_1^{1,-2}$.FIGURE 19. An upper bound for the \mathcal{L}^* -invariant of $9_1^{1,-2}$.

FIGURE 20. A tri-plane diagram of 10_1^1 .FIGURE 21. An upper bound for the \mathcal{L} -invariant of 10_1^1 .FIGURE 22. An upper bound for the \mathcal{L}^* -invariant of 10_1^1 .

FIGURE 23. A tri-plane diagram of 10_3 .FIGURE 24. An upper bound for the \mathcal{L} -invariant and the \mathcal{L}^* -invariant of 10_3 .

FIGURE 25. A tri-plane diagram of $10_1^{0,0,1}$.FIGURE 26. An upper bound for the \mathcal{L} -invariant of $10_1^{0,0,1}$.FIGURE 27. An upper bound for the \mathcal{L}^* -invariant of $10_1^{0,0,1}$.

FIGURE 28. A tri-plane diagram of $10_1^{-2,-2}$.FIGURE 29. An upper bound for the \mathcal{L} -invariant of $10_1^{-2,-2}$.FIGURE 30. An upper bound for the \mathcal{L}^* -invariant of $10_1^{-2,-2}$.